Basal-subtype and MEK-PI3K feedback signaling determine susceptibility of breast cancer cells to MEK inhibition

Olga K. Mirzoeva[1], Debopriya Das[2], Laura M. Heiser[2], Sanchita Bhattacharya[2], Doris Siwak[3], Rina Gendelman, [1]Nora Bayani[2], Nicholas J. Wang[2], Richard M. Neve[2], Bahram Parvin[2], Zachary Knight[4], Heidi S. Feiler[2], Philippe Gascard[2], Paul T. Spellman[2], Kevan M. Shokat[4], Andy Wyrobek[2], Mina J. Bissell[2], Frank McCormick[5], Wen-Lin Kuo[2], Gordon B. Mills[3], Joe W. Gray[2], and W. Michael Korn[1,6,7]

[1]Division of Gastroenterology, Department of Medicine, University of California, San Francisco, CA, USA
[2]Lawrence Berkeley National Laboratory, Life Sciences Division, Berkeley, CA, USA
[3]Department of Systems Biology, MD Anderson Comprehensive Cancer Center, University of Texas, Houston, TX, USA
[4]Department of Cellular and Molecular Pharmacology, University of California, San Francisco, CA, USA
[5]Helen Diller Family Comprehensive Cancer Center, University of California San Francisco, CA
[6]Divisions of Gastroenterology and Hematology/Oncology, Department of Medicine, University of California, San Francisco, CA, USA

[7] Corresponding author:

W. Michael Korn, M.D.
Associate Professor of Medicine In Residence
UCSF Divisions of Gastroenterology and Medical
2340 Sutter St.
San Francisco, CA 94115
USA

Phone office: (415) 502 2844
Phone lab: (415) 476 0137
FAX: (415) 502 4787
Email: mkorn@cc.ucsf.edu

Abstract
Specific inhibitors of MEK have been developed that efficiently inhibit the oncogenic RAF-MEK-ERK pathway. We employed a systems-based approach to identify breast cancer subtypes particularly susceptible to MEK inhibitors and to understand molecular mechanisms conferring resistance to such compounds. Basal-type breast cancer cells were found to be particularly susceptible to growth-inhibition by small-molecule MEK inhibitors. Activation of the PI3 kinase pathway in response to MEK inhibition through a negative MEK-EGFR-PI3 kinase feedback loop was found to limit efficacy. Interruption of this feedback mechanism by targeting MEK and PI3 kinase produced synergistic effects, including induction of apoptosis and, in some cell lines, cell cycle arrest and protection from apoptosis induced by proapoptotic agents. These findings enhance our understanding of the interconnectivity of oncogenic signal transduction circuits and have implications for the design of future clinical trials of MEK inhibitors in breast cancer by guiding patient selection and suggesting rational combination therapies.

Introduction

The RAS-RAF-MEK-ERK and PI3 kinase-PTEN-AKT signaling pathways play central roles in the signal transduction networks promoting tumor initiation and tumor progression. This is highlighted by the high frequency of mutations of *RAS*, *RAF*, *PI3KCA*, *AKT*, *PTEN* as well as amplification of *AKT* present in a broad spectrum of human malignancies[1-5]. Since signal transduction networks integrate multiple up-stream inputs, targeting pathways down-stream of the receptors could conceivably result in greater therapeutic efficacy and broader applicability. For example, abolishing signal transduction through MEK offers the potential advantage of inhibiting both proliferation-promoting and anti-apoptotic signals originating from either activated cell surface receptors or mutant *Ras* and *B-Raf*. In breast cancer, activation of the Raf-MEK-ERK signaling cascade is associated with increased metastasis risk[6]. Furthermore, cross-talk between the RAF-MEK-ERK pathway and the estrogen receptor (ERα) might mediate tamoxifen resistance[7]. While these findings validate the RAF-MEK-ERK pathway as a therapeutic target in breast cancer, clinical studies of MEK inhibitors have demonstrated only limited anti-tumor activity[8,9]. The mechanisms underlying the poor clinical response to inhibition of MEK remain unclear and no markers of susceptibility or resistance to MEK inhibitors suitable for guiding patient selection have been identified.

The availability of advanced genomic and proteomic technologies has facilitated capturing the complex molecular responses to defined stimuli at a systems level. For example, Reverse Phase Protein Array (RPPA) represents an emerging proteomic technology allowing for comprehensive assessment of signal transduction pathways at the protein and phospho-protein level[10,11]. Here, we pursued a systems-based experimental strategy to create an in-depth understanding of the responses of breast cancer cells to MEK inhibition. We found basal-type breast cancers to be particularly sensitive to such agents. Furthermore, a potent negative feedback loop between the RAF-MEK-ERK and PI3 kinase pathways was discovered, which counteracts effects of MEK inhibition on cell cycle and apoptosis-induction. In agreement with this finding, combined treatment with MEK and PI3 kinase inhibitors resulted in marked tumor cell growth inhibition.

Results

Basal-type breast cancer cell lines are particularly susceptible to MEK-inhibition

We ascertained the effect of pharmacological inhibition of MEK in a large panel of breast cancer cell lines that was described before[12]. Cells were treated with the specific MEK inhibitors CI1040 or U0126 and cell viability was determined. A wide spectrum of growth inhibition was observed. For U0126, the GI50 ranged from 0.8 μM (HCC1187 cells) to 60 μM (MDAMB231 cells) while the GI50 for CI1040 treated cells ranged from 0.8 μM (SUM229PE) to 33 μM (MDAMB231 cells). Compared with luminal type cell lines, basal-type breast cancer cells demonstrated more frequent growth inhibition in response to MEK inhibitor treatment, in particular following treatment with CI1040 (Figure 1, Supplemental Materials). For the majority of cell

lines however, the LC50 was not reached. Only nine cell lines treated with U0126 and eight cell lines treated with CI1040 were killed at concentrations of equal or less than 50 μM and 25 μM, respectively (data not shown).

MAPK pathway genes predict responsiveness to MEK inhibitors in human breast cancer cell lines and tumors

To identify genes and pathways predicting sensitivity to MEK inhibitors, we performed a correlation analysis of mRNA expression data from the cell line panel with the abovementioned growth-inhibition data. The previously reported mRNA microarray data of the cell line set were utilized[12]. Using the SplineMarker algorithm, we identified 1548 (883) gene transcripts associated with sensitivity to CI1040 (UO126), and 790 (671) transcripts were associated with resistance. Among these, 292 and 127 predictors, associated with sensitivity and resistance respectively, were common to both drugs. Pathway enrichment analysis revealed that the predictive mRNA markers are significantly enriched in four pathways for U0126 and eight for CI1040 (Supplemental Table 2). These included ERK/MAPK Signaling, Purine Metabolism, p53 Signaling, and Metabolism of Xenobiotics by Cytochrome P450. Genes involved in ERK/MAPK signaling were predictive of sensitivity, while PI3K pathway components were associated with resistance to MEK inhibitors (Figure 2). Hierarchical cluster analysis revealed that genes predictive of susceptibility to MEK inhibitors were relatively over-expressed in basal-type cell lines while resistance markers were highly expressed in luminal cells (Figure 2). A multivariate model of response to CI1040 consisting of 26 mRNA predictors from the Ingenuity MAPK pathway gene set were confirmed as involved in this pathway by at least one additional database (KEGG, Biocarta, GeneGo, and GSEA). We trained the model on a randomly selected set of 31 breast cancer cell-lines, and tested the accuracy of the model on the remaining 10 cell-lines. The best model consisted of only one gene (RAC2). The sensitivity predicted by the model was strongly correlated with the measured sensitivity on the test set: r =0.69 (p = 0.027). We applied this *in vitro* molecular predictor to forecast sensitivity to CI1040 of previously reported 118 tumors[13]. The model predicted that the basal tumors are more sensitive to CI1040 than the luminal tumors. The difference in predicted sensitivities between these two groups was statistically significant (p = 6.7e-03).

Protein predictors of susceptibility to MEK inhibition

Since the MAPK pathway is regulated predominantly through protein modification, in particular phosphorylation, we ascertained the differences in protein expression levels as predictors of susceptibility to MEK inhibition in the panel of 53 breast cancer cell lines by performing Western blot analysis for the detection of 64 proteins. In addition, expression and phosphorylation of 34 proteins was assessed by RPPA technology. Fifteen phosphoproteins common to both approaches were included in the analysis. The correlation between protein expression levels in the breast cancer cell panel and GI50 of CI1040 as well as U0126 was calculated using SplineMarker (Supplemental Table 3). Ten proteins were significantly correlated with susceptibility to MEK inhibition for both drugs (Supplemental Table 4). Cytokeratin 5/6, a well established marker for the basal breast cancer subtype, showed the strongest

correlation with GI50 of the MEK inhibitors. Expression of cytokeratin 18 and ERα, both luminal subtype markers, was correlated with resistance to MEK inhibitors. These findings clearly support the notion that basal-type breast cancer cell lines are particularly susceptible to MEK inhibitors.

Temporal proteomic analysis reveals a novel negative feedback loop between MEK and PI3 kinase, mediated by the EGF receptor

To further understand the response of signal transduction pathways to MEK inhibition, we analyzed temporal changes in protein expression and phosphorylation by RPPA technology. As expected, a strong reduction in phosphorylated ERK levels in response to MEK inhibitor treatment was observed, along with down-regulation of effectors of ERK, such as cyclin D1 (Figure 3A, B). Additionally, EGF treatment induced phophorylation of the EGF receptor and down-stream effectors, such as Akt. Unexpectedly, MEK inhibition led to markedly enhanced phosphorylation of EGFR and activation of the PI3 kinase pathway, as determined by phospho-Akt at S473. We confirmed key findings by conventional Western blotting in MDAMB231 and T47D cells using two different MEK inhibitors, CI1040 and U0126 (Figure 3C, Figure 5A and data not shown), demonstrating that activation of Akt in response to MEK inhibition is not limited to a single cell line or a result of off-target effects of one drug. Over-activation of EGFR and Akt was most striking in the presence of EGF in the medium, as determined by Western blot analysis (Figure 4). To test whether the increased phosphorylation of Akt was dependent on over-activation of EGFR, we treated MDAMB231cells with the specific EGF receptor inhibitor gefitinib in the presence or absence of CI1040. We found that in low serum conditions in the presence of EGF, MEK inhibitor induced activation of Akt was fully abolished by the treatment with gefitinib. In 10% serum, the effect of gefitinib was still observed, although to a lesser degree. To rule out that MEK-dependent activation of Akt being a cell line specific phenomenon, we assessed pAKT in eight cell lines treated with CI1040 under low serum conditions and found increased pAkt levels in five cell lines: MDAMB231, T47D, HS578T, MDAMB175, and Sum149 (Figure 5A and data not shown). Thus, a negative regulatory feedback loop exists between MEK and Akt that depends on activation of the EGF receptor and thus represents a signal-amplifying mechanism (Figure 5B,C).

Synergistic cellular effects of inhibition of MEK and PI3 kinase in breast cancer cells with feedback activation of Akt

Since suppression of apoptosis is among the known biological effects mediated by the PI3 kinase pathway, we hypothesized that the feedback activation of the pathway in response to MEK inhibition contributes to resistance of breast cancer cells to MEK inhibitors. We therefore hypothesized that inhibitors of PI3 kinase should synergize with MEK inhibitors in cell lines demonstrating feedback activation of Akt. We tested this, using inhibitors of PI3 kinase specific for the p110α isoform, PIK90 and PI103 [14]. This PI3 kinase isoform is frequently mutated in cancer and a crucial signal transducer in cancer cells [15-17]. Synergistic growth inhibition following PI3 kinase and MEK inhibition occurred in four cell lines out of eleven tested (Figure 5D). The calculated Combination Index (CI) values ranged from 0.259 (HS578T) to

0.742 (SUM149 cells), which are considered strong, and moderate synergism, respectively. These cell lines had demonstrated strong activation of Akt following MEK inhibition. However, only MDAMB175 and SUM149 cell lines demonstrated an increase in apoptosis rates when treated with a combination of MEK and PI3 kinase inhibitors (Supplemental Table 5 and data not shown). In contrast, in other cell lines, including MDAMB231 cells, the combination of CI1040 or UO126 with PI3 kinase inhibitors induced a complete G1 arrest (Figure 6A). Interestingly, cell lines responding with apoptosis to the dual-inhibitor treatment harbor wild-type p53 while those demonstrating synergistic effects on cell cycle distribution contain mutant p53.

Cooperative G1 growth arrest results from synergistic inhibition of cyclin D1

We sought to further understand the cell cycle effects induced by inhibition of MEK and PI3 kinase and analyzed the response of proteins down-stream of these molecules. This analysis included mTOR kinase, an important regulator of protein translation, It is required for activation of S6 kinase and 4E-BP1, which regulates cap-dependent mRNA translation. Despite the inhibition of MEK by CI1040 in MDAMB231 cells, phosphorylation of both pS6 kinase and p4E-BP1 did not change (Figure 6B) while inhibition of PI3 kinase with PIK90 led to a significant reduction in S6K phosphorylation and a moderate inhibition of 4E-BP1 phosphorylation. The combination of CI1040 and PIK90, in contrast, further inhibited activation of S6 kinase and caused a marked decrease in 4E-BP1 phosphorylation (Figure 6B). Expression of Cyclin D1, a target of translational regulation by the mTOR pathway[18], was slightly reduced after MEK inhibition while treatment with PIK90 led to increased levels at the 24 hour time point. In contrast, the combination of both inhibitors resulted in a strong down-regulation of cyclin D1 protein, which was paralleled by reduction in the corresponding mRNA levels. (Figure 6C). Thus, regulation of cyclin D1 gene expression drives the expression levels of cyclin D1 protein, while translational regulation play a minor role in this context. Indeed, knock-down of cyclin D1 expression by siRNAs resulted in G1 arrest (data not shown), demonstrating the impact of cyclin D1 levels on G1/S cell cycle progression in these cells. Based on these data it appears that cyclin D1 represents a major intersection point between the Raf-MEK-ERK and PI3 kinase pathways, mediating cell cycle arrest in response to pharmacological inhibition of these pathways. Interestingly, dual inhibition of PI3 kinase and mTOR (with PIK90 and rapamycin or the dual PI3 kinase/mTOR inhibitor PI103), which acts down-stream of both, the MAPK and PI3 kinase pathways, was not sufficient to induce a significant reduction of cyclin D1 protein or mRNA levels (Figure 6B/C). Thus, reduction of MEK-dependent and mTOR-independent regulatory factors is required for the observed repression of cyclin D1.

MEK inhibition counteracts apoptotic cell death induced by camptothecin

Since it has been described by others that cells arresting in the G1 phase of the cell cycle might be protected from apoptosis induction, we assessed whether MEK inhibition would alter sensitivity to apoptosis induced by chemotherapy in MDAMB231 cells. As shown in Figure 6D, we treated MDAMB231 cells for one or 24 hours with CI1040 or DMSO (control) before adding the chemotherpeutic agent

camptothecin which strongly induces apoptosis in these cells. In agreement with our prediction, apoptosis induction was inhibited after one hour of CI1040 pretreatment. After 24 hours of pretreatment with CI1040, the proaptotic activity of camptothecin was completely abolished. Thus, MEK inhibition not only did not induce apoptosis but acted as a cytoprotective when breast cancer cells were treated with proapoptotic agents.

Discussion

In this study, we examine the molecular features of breast cancer cells that determine sensitivity to pharmacological inhibition of the MEK-ERK signal transduction pathway. We used a large set of breast cancer cell lines as a model system. Previously, we demonstrated that these cell lines retain molecular abnormalities characteristic for human breast cancers[12] and we utilized this system to define molecular predictors for susceptibility to lapatinib, and for EGFR and Her2/Neu. These were validated in a clinical study of lapatinib in combination with paclitaxel (manuscript in preparation). Similar approaches were previously employed to identify molecular signatures of susceptibility to conventional chemotherapeutic agents[19]. Thus, the validity of cell-line based approaches for the preclinical development and optimization of treatment strategies using targeted therapeutics has been well established.

A major finding of this study is the particular sensitivity of basal-type cell lines to inhibitors of MEK. This has implications for our understanding of the role of the MAPK pathway in basal-type breast cancer as well as for the further development of MEK inhibitors clinically. The predictive nature of basal-type features was strongly supported by our analysis of correlation of protein expression patterns and sensitivity to MEK inhibitors. The most predictive protein marker was cytokeratin 5/6, a well established marker of basal-type breast cancer[20-22]. Additional sub-type defining markers were found to be correlated with response to MEK inhibitors (EGFR with sensitivity, ERα, and cytokeratin 18 with resistance). High expression levels of EGFR and lack of expression of ERα and CK18 are characteristic for basal-type breast cancers[23]. Our analysis of gene-expression predictors of response revealed a strong enrichment of genes encoding for MAPK pathway components. Furthermore, we found increased expression of these gene predictors in basal-type cell lines, demonstrating that basal-type cells utilize this pathway to a greater extent than luminal cells and depend on its activity for proliferation. Interestingly, gene expression of the Rho-like GTPase RAC2 was highly predictive of responsiveness to MEK inhibition in breast cancer cell lines and in human tumors. Activation of the MAPK pathway has been demonstrated as a central feature of basal-type breast cancers[24]. Over-expression of EGFR, amplification and mutation of the KRAS oncogene, and over-expression of αB-crystallin have been shown to lead to activation of this pathway in basal-type breast cancer. αB-crystallin is a MEK-activating heat-shock protein that is over-expressed in basal-type breast cancers and associated with poor outcome[25]. Luminal type cells might utilize the MEK-ERK pathway to a lesser extent and appear to be more dependent on the PI3 kinase

pathway, demonstrated by the preferential occurrence of PI3 kinase mutations in this subtype[26] and our finding that Akt protein levels predict resistance to MEK inhibitors.

The role of the PI3 kinase pathway in conferring resistance to MEK inhibitors is highlighted by our discovery of a negative feedback loop activating Akt in response to MEK inhibition in an EGFR-dependent fashion, thus amplifying EGF signals (Figure 5B,C). Crosstalk between the MAPK and PI3 kinase pathways has been described before. A negative feedback loop has been demonstrated from ERK to the Grb2-associated Binder 1 protein (GAB1), a scaffold protein that propagates EGFR signals to the PI3 kinase and the RAS/MAPK pathways[27,28]. Since the PI3 kinase pathway is a known promoter of the cell cycle and negative regulator of apoptosis we reasoned that feedback activation of Akt could counteract therapeutically relevant effects of MEK inhibition. Indeed, dual-inhibition of MEK and PI3 kinase led to synergistic down-regulation of cyclin D1 mRNA and protein levels, as well as growth inhibition in cell lines demonstrating strong feedback activation of Akt following MEK inhibition. The role of cyclin D1 in mediating efficacy of MEK inhibitors is further highlighted by our finding that cyclin D1 protein levels were correlated with resistance to MEK inhibition while levels of GSK3 (a negative regulator of cyclin D1), were correlated with sensitivity to MEK inhibitors. Only a subset of our cell lines responded with cell killing to the dual inhibition while the remainder of cell lines demonstrated synergistic inhibition of the cell cycle. Similar observations were demonstrated by others previously[29]. It is conceivable that the reduced levels of E2F1 as a consequence of loss of cyclin D1 expression could result in protection from apoptosis since known E2F1-dependend proapoptotic genes exist that are inhibited by PI3 kinase[30]. The E2F1-driven apoptotic mechanism is p53 dependent. Interestingly, wild-type p53 is present in cell lines undergoing apoptosis following MEK/PI3 kinase inhibition while p53-mutant cell lines demonstrated synergistic cell cycle arrest. Moreover, in MDAMB231 cells, protection from apoptosis resulted from MEK inhibition in cells treated with camptothecin. These findings suggest that MEK inhibition might have anti-apoptotic effects and thus counteract potential therapeutic effects of other agents administered in combination.

These results are relevant for the design of future clinical trials. The MEK inhibitors CI1040 and AZD6244 have demonstrated only modest anti-tumor activity in early clinical trials[8,9]. In one study that included breast cancer patients, tumor biopsies demonstrated reduction of pERK levels and reduction of the proliferation marker KI-67 in tumor biopsies[9]. This finding corresponds well with our observation of predominant cell-cycle effects of MEK inhibitors in breast cancer. Our findings suggest focusing further development efforts of MEK inhibitors in breast cancer on patients with basal-type cancers, which are representing about 15% of all sporadic and greater than 60% of BRCA1-related breast cancers[31,32]. Currently, treatment options for these patients are limited and MEK-inhibitors might represent a promising therapy. Furthermore, inhibiting the MEK-EGFR-PI3 kinase feedback loop is likely to result in therapeutic synergism, in particular in cases with wild-type p53.

Materials and Methods

Reagents.

Chemical synthesis and characterization of PI3-K inhibitors PI103 and PIK90 are described in: [14]. The following other reagents were used: Rapamycin (Calbiochem), U0126 (Promega), EGF (Millipore). CI1040 (PD 184352) was kindly provided by Dr Jenny Bain, University of Dundee, UK. All drugs were diluted in DMSO except for PIK90 which was diluted in DMSO : H2O 1:1 (v/v). The list of antibodies used in this study is provided in Supplemental Table 6.

Cell culture.

Breast cancer cell lines used in this study were described in detail previously[12]. The serum used throughout the course of this study was FetalClone III (HyClone), which is not supplemented with EGF.

Cell growth inhibition assay and data analysis.

Cell viability was determined using the CellTiter-Glo (CTG) assay (Promega, Madison, WI). Cells were treated with MEK inhibitors CI1040 or U0126 dissolved in DMSO. Nine dilutions of each drug were made in 1:5 serial dilution. The cell growth was determined using CTG assay at days 0 and 3 of drug exposure. Growth inhibition was calculated as described by the NCI/NIH DTP (http://dtp.nci.nih.gov/branches/btb/ivclsp.html)[33]. The 50% growth inhibiting concentration (GI50), total growth inhibiting concentration (TGI) and 50% lethal concentration (LC50) were calculated using a standardized algorithms. Drug combination studies were designed according to Chou and Talalay [34]. Calcusyn software (Biosoft, Ferguson, MO) was used to calculate the combination index (CI). CI < 1 indicates synergy, a CI about 1 shows an additive effect, and CI > 1 indicates antagonism. Combined drugs were used at fixed molar ratios.

Identification of predictors of response to MEK inhibition based on mRNA expression

SplineMarker (a variant of the linear splines method allowing for modeling of non-linear relationships between molecular markers and response[35]) was used to identify the mRNA predictors of response to the MEK inhibitors CI1040 and UO126 using existing mRNA expression profiles from 51 breast cancer cell lines [12]. A false discovery rate of 10% was used to identify transcripts associated with responsiveness to MEK inhibition. Baseline expression data for the MAPK-related gene predictors were hierarchically clustered with xcluster (http://fafner.stanford.edu/~sherlock/cluster.html) using a non-centered metric and pearson correlation. We visualized the data with Java TreeView (http://jtreeview.sourceforge.net/). Model parameters are learnt by performing least squares fit between the molecular profile and sensitivity profile for each molecular variable. The final model is determined via leave-one-out cross-validation. The goodness of fit is assessed by evaluating a p-value corresponding to the F-statistic for the fit[35]. p-values are corrected for multiple hypotheses testing using the false discovery rate method[36]. Ingenuity pathway enrichment analysis was performed

using the Ingenuity Knowledge Base Database (http://www.ingenuity.com/) separately for the sensitivity and resistance mRNA predictors. p-values were computed using Fisher's exact test , with Affymetrix HT_Hgu133A as a reference set. We used a threshold of $p < 0.01$ to identify significant pathways.

Identification of protein predictors of response to MEK inhibitors
Protein expression profiles were generated in 35 breast cancer cell lines using conventional Western blot analysis for the detection of 64 proteins. In addition, expression of 34 proteins was assessed by reverse-phase protein lysate array (RPPA). Proteins predicting response to MEK inhibition were identified using the SplineMarker algorithm.

Proteomic analysis of MEK inhibition by Reversed-Phase Protein Array (RPPA).
MDAMB231 cells were transferred to low serum conditions 24h prior to treatment. The cells were pre-treated with U0126 (10uM) or DMSO (control), for 30 min after which EGF was added at a final dose of 10 ng/ml. Protein lysates were collected at 1h, 4h and 24h after EGF stimulation, denatured in SDS sample buffer and spotted onto nitrocellulose-coated FAST® slides (Whatman, Floram Park, NJ) using a GeneTAC™ G3 arrayer (Genomic Solutions, Ann Arbor, MI). Proteins were dected using a set of validated antibodies (Supplemental Metarials) and quantified as described before[37-39].

Preparation of protein lysates and Western blots.
The cells were treated with drugs either in low serum or in full serum conditions as indicated in the figures. For the low serum conditions cells were washed in the media containing 0.1% FBS and incubated in this media for 24h. Drugs or DMSO (control), were added directly to this media and 30 min later EGF was added at a final dose of 10 ng/ml. Cells were harvested at time intervals post EGF stimulation. For the full serum conditions, cells were grown in their normal growth media and at 48h after plating were treated with the drugs. Protein lysates were prepared from cells at 70%–90% confluency. The cells were washed in ice-cold PBS, then extracted in the lysis buffer containing: 1% Triton X-100, 50 mM HEPES (pH 7.5), 150 mM NaCl, 25 mM β-glycerophosphate, 25 mM NaF, 5 mM EGTA, 1 mM EDTA, protease cocktail inhibitor set III, phosphatase cocktail inhibitor set II (Calbiochem). The lysates were clarified by centrifugation for 13000 rpm for 10 min on ice and frozen at −80°C. Protein concentrations were determined using the BCA protein assay kit (Pierce Biotechnology, Rockford, IL). 20 µg of protein extract per lane was electrophoresed, transferred to PVDF membranes (Millipore), and probed with specific antisera using standard techniques. Bound antibodies on immunoblots were detected by chemiluminescence (ECL, Amersham).

Cell cycle and apoptosis analyses.
Cells were treated with drugs 24 hours after plating and harvested for apoptosis or cell cycle assays at 72h post-treatment. Apoptosis was measured in live cells by Annexin V-FITC and propidium iodide (PI) labeling using Apoptosis detection kit I (BD Pharmingen) and quantified by Flow Cytometry (FACS Calibur, BD) with

CellQuest software. For cell cycle analysis, cells were fixed in 70% ethanol, treated with PI (30 µg/ml) and RNase A (100 µg/ml), and subjected to FACS analysis. Data analysi was performed using ModFit LT cell cycle analysis software (Verity Software House, Topsham, ME). All treatments were done in triplicates and at least 40,000 cells were acquired from every sample for the FACS analysis.

Acknowledgement
This project was supported by the Director, Office of Science, Office of Basic Energy Sciences, of the U.S. Department of Energy under Contract No. DE-AC02-05CH11231, by the National Institutes of Health, National Cancer Institute grantsP50 CA 58207, U54 CA 112970 (to JWG) and P30 CA82103 (to FM).

Figure Legends

Figure 1. Comparison of sensitivity of breast cancer cell lines to MEK inhibitor CI1040. 46 basal or luminal breast cancer cell lines were treated with increasing doses of CI1040 and cell viability was assessed at 0h (time of drug addition) and at 72h after treatment. GI50 was calculated from the dose-response curves as described in Experimental Procedures. Data are presented as GI50 (M) of cell lines in the order of most sensitive to most resistant (from left to right).
Red and green bars represent basal and luminal cellular phenotype, respectively. All data for GI50, TGI, LC50 for CI1040 and U0126 response of cell lines are summarized in Supplemental Table 1.

Figure 2. Breast cancer cell lines can be hierarchically clustered according to their expression of the MAPK-related gene predictors. Each row represents the relative transcript abundance (in log2 space) for one gene; each column represents data from one cell line. Expression of genes in the upper panel predict sensitivity to MEK inhibitors while expression of those in the lower panel predict resistance. Within each panel, genes are ordered by q-value. In the upper panel, the most significant predictors are at the top; in the lower panel, the most significant predictors are at the bottom. In the tree, yellow end-nodes denote basal cell lines and pink end-nodes denote luminal cell lines.

Figure 3 – Proteomic analysis of MEK inhibition in breast cancer cells.
A: Heat-map of protein and phosphoprotein expression profiles. MDAMB231 cells were treated with MEK inhibitor U0126 (10uM) as described in experimental procedures, 30 min later they were stimulated with EGF (10ng/ml). The protein lysates were collected at 1, 4 and 24 hours post EGF addition and analyzed by RPPA. Values are expressed as Log2 fold difference from control (untreated) samples at each time point.
B: Relative expression changes of AKTpS473, EGFRpY1068, pMAPK, and CCND1 as detected by RPPA. Grey bars: EGF treatment, black bars: EGF + U0126 treatment, control = 0. Values for phospho-proteins were normalized by corresponding total protein levels.
C: Conventional Western blot analysis of p-Akt and p-Erk (pMAPK) expression in response to U0126 treatment in T47D and MDAMB231 cell lines. Cells were treated with MEK inhibitor in the same conditions as for RPPA experiment and the protein lysates were collected at 1h and 4h post EGF stimulation.

Figure 4. Western blot analysis of the biochemical response of MDAMB231 cells treated with MEK inhibitor CI1040, EGFR inhibitor Gefitinib or their combination in low (0.1% FBS) and full (10% FBS) serum conditions. Cells were harvested at 4h post drug treatment. In low serum conditions and in the presence of EGF, MEK inhibition results in strong phospho-EGFR and phospho-Akt upregulation, this is abrogated by EGFR inhibitor.

Figure 5. Synergistic response of breast cancer cell lines to a combination of MEK and PI3K inhibitors correlates with their upregulated p-Akt status induced by MEK inhibition.
A. Western blot analysis of p-Akt and p-Erk expression in response to CI1040 treatment in four breast cancer cell lines: MDAMB231, MDAMB175, HS578T, SUM149. The cells were treated with MEK inhibitor in low serum conditions, in 30 min they were stimulated with EGF and the protein lysates were collected at 4h post EGF.
B,C. Schematic summary of the Ras-Raf-MEK-ERK and PI3 kinase pathway interconnectivity in the absence (B) and presence (C) of MEK inhibitors.
D. Synergistic effect of combination of MEK and PI3K inhibitors on cell viability of cell lines displaying MEKi– induced Akt phosporylation. Dose/effect curves for single inhibitors CI1040 and PIK90 and their combinations at fixed molar ratio are presented. Cell viability was measured at 72h post treatment with the drugs using ATP-based cell viability assay (Promega). Relative cell viability of drug-treated cells was calculated as a fraction of control. The results are the mean+/- SD from triplicates. Combination indexes (CI) at 50% dose-response are calculated using Calcusyn Software.

Figure 6. Biologic effects of MEK inhibitors in combination with PI3 kinase inhibitors and camptothecin.
A. FACS-based analysis was used to determine percentage of MDAMB231 cells in G1, S and G2 phases of the cell cycle at 72 h post treatment with the single drugs and with their combinations at indicated doses. Whereas PI3K inhibitors PIK90 and PI103 do not affect cell cycle distribution, their addition to MEK inhibitors CI1040 or U0126 results in complete G1 arrest. The data are expressed as the mean +/- SD from duplicates, for each duplicate 40,000 cells were acquired. The result was confirmed in 2 independent experiments.
B. Analysis of the response of MDAMB231 cells treated with MEK inhibitor CI1040, PI3K and/or mTOR inhibitors: PIK90, PI103, rapamycin and with the drug combinations. Representative Western blot analysis of MDAMB231 cells treated with the indicated drugs and their combinations for 4h or 24h. The cells were treated with drugs in full serum conditions and were harvested at 4h- and 24h post drug addition for protein and RNA isolation.
C: Cyclin D1 gene expression changes induced by the same drug treatments as in the upper panel: 1- control, 2- CI1040 (5uM), 3- PIK90 (5uM), 4- PI103 (0.5 uM), 5- CI1040 + PI103, 6- CI1040 + PIK90, 7- CI1040 + PIK90 + rapamycin, 8- PIK90 + rapamycin, 9- rapamycin (5 nM). Gene expression was analyzed by TaqMan assay; the results are averaged from duplicates. Relative Cyclin D1 expression is presented as the percentage of that of control (untreated) cells.
D. G1 arrest induced by MEK inhibition rescues the cells from apoptosis induced by cytotoxic agent. MDAMB231 cells were treated with camptothecin (2.5uM) for 48h, what resulted in 20% of apoptotic cells. Pre-treatment of cells with CI1040 for 1h reduced the amount of apoptotic cells, whereas pretreatment of cells for 24h completely eliminated apoptosis induced by camptothecin. The data are expressed

as the mean +/- SD from duplicates, for each duplicate 40,000 cells were acquired. The results were confirmed in 2 independent experiments.

References

1. Saal, L.H.*, et al.* PIK3CA mutations correlate with hormone receptors, node metastasis, and ERBB2, and are mutually exclusive with PTEN loss in human breast carcinoma. *Cancer research* **65**, 2554-2559 (2005).
2. Perez-Tenorio, G.*, et al.* PIK3CA mutations and PTEN loss correlate with similar prognostic factors and are not mutually exclusive in breast cancer. *Clin Cancer Res* **13**, 3577-3584 (2007).
3. Berns, K.*, et al.* A functional genetic approach identifies the PI3K pathway as a major determinant of trastuzumab resistance in breast cancer. *Cancer cell* **12**, 395-402 (2007).
4. Rochlitz, C.F.*, et al.* Incidence of activating ras oncogene mutations associated with primary and metastatic human breast cancer. *Cancer research* **49**, 357-360 (1989).
5. Brugge, J., Hung, M.C. & Mills, G.B. A new mutational AKTivation in the PI3K pathway. *Cancer cell* **12**, 104-107 (2007).
6. Adeyinka, A.*, et al.* Activated mitogen-activated protein kinase expression during human breast tumorigenesis and breast cancer progression. *Clin Cancer Res* **8**, 1747-1753 (2002).
7. Thomas, R.S., Sarwar, N., Phoenix, F., Coombes, R.C. & Ali, S. Phosphorylation at serines 104 and 106 by Erk1/2 MAPK is important for estrogen receptor-{alpha} activity. *J Mol Endocrinol* **40**, 173-184 (2008).
8. Rinehart, J.*, et al.* Multicenter phase II study of the oral MEK inhibitor, CI-1040, in patients with advanced non-small-cell lung, breast, colon, and pancreatic cancer. *J Clin Oncol* **22**, 4456-4462 (2004).
9. Adjei, A.A.*, et al.* Phase I pharmacokinetic and pharmacodynamic study of the oral, small-molecule mitogen-activated protein kinase kinase 1/2 inhibitor AZD6244 (ARRY-142886) in patients with advanced cancers. *J Clin Oncol* **26**, 2139-2146 (2008).
10. Nishizuka, S.*, et al.* Proteomic profiling of the NCI-60 cancer cell lines using new high-density reverse-phase lysate microarrays. *Proceedings of the National Academy of Sciences of the United States of America* **100**, 14229-14234 (2003).
11. Hu, J.*, et al.* Non-parametric quantification of protein lysate arrays. *Bioinformatics (Oxford, England)* **23**, 1986-1994 (2007).
12. Neve, R.M.*, et al.* A collection of breast cancer cell lines for the study of functionally distinct cancer subtypes. *Cancer cell* **10**, 515-527 (2006).
13. Chin, K.*, et al.* Genomic and transcriptional aberrations linked to breast cancer pathophysiologies. *Cancer cell* **10**, 529-541 (2006).
14. Knight, Z.A.*, et al.* A pharmacological map of the PI3-K family defines a role for p110alpha in insulin signaling. *Cell* **125**, 733-747 (2006).
15. Campbell, I.G.*, et al.* Mutation of the PIK3CA gene in ovarian and breast cancer. *Cancer research* **64**, 7678-7681 (2004).
16. Samuels, Y.*, et al.* High frequency of mutations of the PIK3CA gene in human cancers. *Science* **304**, 554 (2004).

17. Shayesteh, L.*, et al.* PIK3CA is implicated as an oncogene in ovarian cancer. *Nature genetics* **21**, 99-102 (1999).
18. Rosenwald, I.B.*, et al.* Eukaryotic translation initiation factor 4E regulates expression of cyclin D1 at transcriptional and post-transcriptional levels. *The Journal of biological chemistry* **270**, 21176-21180 (1995).
19. Potti, A.*, et al.* Genomic signatures to guide the use of chemotherapeutics. *Nat Med* **12**, 1294-1300 (2006).
20. Perou, C.M.*, et al.* Molecular portraits of human breast tumours. *Nature* **406**, 747-752. (2000).
21. Sorlie, T.*, et al.* Gene expression patterns of breast carcinomas distinguish tumor subclasses with clinical implications. *Proceedings of the National Academy of Sciences of the United States of America* **98**, 10869-10874 (2001).
22. Bocker, W.*, et al.* Common adult stem cells in the human breast give rise to glandular and myoepithelial cell lineages: a new cell biological concept. *Lab Invest* **82**, 737-746 (2002).
23. Rakha, E.A., Reis-Filho, J.S. & Ellis, I.O. Impact of Basal-like breast carcinoma determination for a more specific therapy. *Pathobiology* **75**, 95-103 (2008).
24. Hoadley, K.A.*, et al.* EGFR associated expression profiles vary with breast tumor subtype. *BMC Genomics* **8**, 258 (2007).
25. Moyano, J.V.*, et al.* AlphaB-crystallin is a novel oncoprotein that predicts poor clinical outcome in breast cancer. *J Clin Invest* **116**, 261-270 (2006).
26. Hollestelle, A., Elstrodt, F., Nagel, J.H., Kallemeijn, W.W. & Schutte, M. Phosphatidylinositol-3-OH kinase or RAS pathway mutations in human breast cancer cell lines. *Mol Cancer Res* **5**, 195-201 (2007).
27. Yu, C.F., Liu, Z.X. & Cantley, L.G. ERK negatively regulates the epidermal growth factor-mediated interaction of Gab1 and the phosphatidylinositol 3-kinase. *The Journal of biological chemistry* **277**, 19382-19388 (2002).
28. Kiyatkin, A.*, et al.* Scaffolding protein Grb2-associated binder 1 sustains epidermal growth factor-induced mitogenic and survival signaling by multiple positive feedback loops. *The Journal of biological chemistry* **281**, 19925-19938 (2006).
29. Torbett, N.E.*, et al.* A chemical screen in diverse breast cancer cell lines reveals genetic enhancers and suppressors of sensitivity to PI3K isotype-selective inhibition. *The Biochemical journal* (2008).
30. Hallstrom, T.C., Mori, S. & Nevins, J.R. An E2F1-dependent gene expression program that determines the balance between proliferation and cell death. *Cancer cell* **13**, 11-22 (2008).
31. Abd El-Rehim, D.M.*, et al.* High-throughput protein expression analysis using tissue microarray technology of a large well-characterised series identifies biologically distinct classes of breast cancer confirming recent cDNA expression analyses. *Int J Cancer* **116**, 340-350 (2005).
32. Lakhani, S.R.*, et al.* Prediction of BRCA1 status in patients with breast cancer using estrogen receptor and basal phenotype. *Clin Cancer Res* **11**, 5175-5180 (2005).

33. Monks, A.*, et al.* Feasibility of a high-flux anticancer drug screen using a diverse panel of cultured human tumor cell lines. *Journal of the National Cancer Institute* **83**, 757-766 (1991).
34. Chou, T.C. & Talalay, P. Quantitative analysis of dose-effect relationships: the combined effects of multiple drugs or enzyme inhibitors. *Adv Enzyme Regul* **22**, 27-55 (1984).
35. Das, D., Nahle, Z. & Zhang, M.Q. Adaptively inferring human transcriptional subnetworks. *Molecular systems biology* **2**, 2006 0029 (2006).
36. Storey, J.D. & Tibshirani, R. Statistical significance for genomewide studies. *Proceedings of the National Academy of Sciences of the United States of America* **100**, 9440-9445 (2003).
37. Tibes, R.*, et al.* Reverse phase protein array: validation of a novel proteomic technology and utility for analysis of primary leukemia specimens and hematopoietic stem cells. *Molecular cancer therapeutics* **5**, 2512-2521 (2006).
38. Sheehan, K.M.*, et al.* Use of reverse phase protein microarrays and reference standard development for molecular network analysis of metastatic ovarian carcinoma. *Mol Cell Proteomics* **4**, 346-355 (2005).
39. Murph, M.M.*, et al.* Individualized molecular medicine: linking functional proteomics to select therapeutics targeting the PI3K pathway for specific patients. *Advances in experimental medicine and biology* **622**, 183-195 (2008).
40. Lacher, M.D.*, et al.* Transforming growth factor-beta receptor inhibition enhances adenoviral infectability of carcinoma cells via up-regulation of Coxsackie and Adenovirus Receptor in conjunction with reversal of epithelial-mesenchymal transition. *Cancer research* **66**, 1648-1657 (2006).

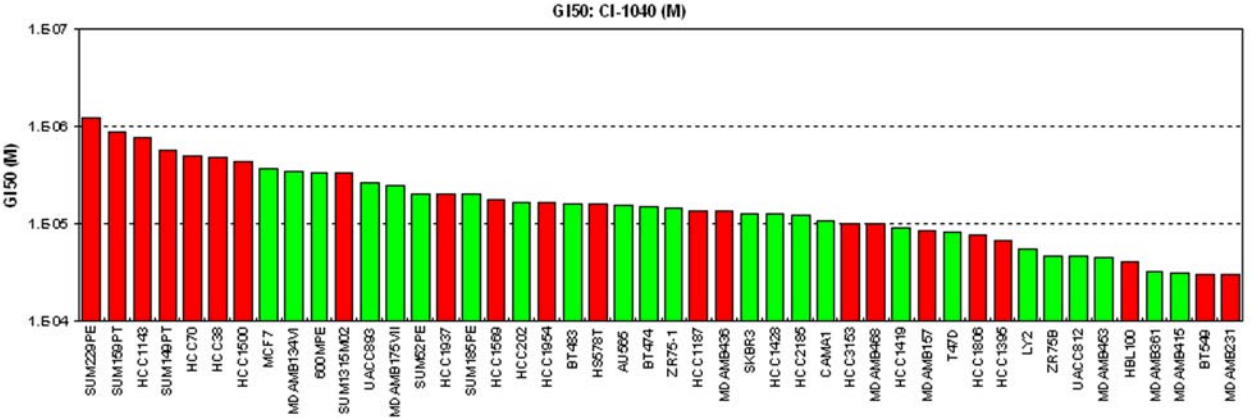
GI50: CI-1040 (M)
GI50 (M)
1.E-07
1.E-06
1.E-05
1.E-04
SUM229PE
SUM159PT
HCC1143
SUM149PT
HCC70
HCC38
HCC1500
MCF7
MDAMB134VI
600MPE
SUM1315MO2
UACC893
MDAMB175VII
SUM52PE
HCC1937
SUM185PE
HCC1569
HCC202
HCC1954
BT483
HS578T
AU565
BT474
ZR75-1
HCC1187
MDAMB436
SKBR3
HCC1428
HCC2185
CAMA1
HCC3153
MDAMB468
HCC1419
MDAMB157
T47D
HCC1806
HCC1395
LY2
ZR758
UACC812
MDAMB453
HBL100
MDAMB361
MDAMB415
BT549
MDAMB231

Figure 1

Figure 2

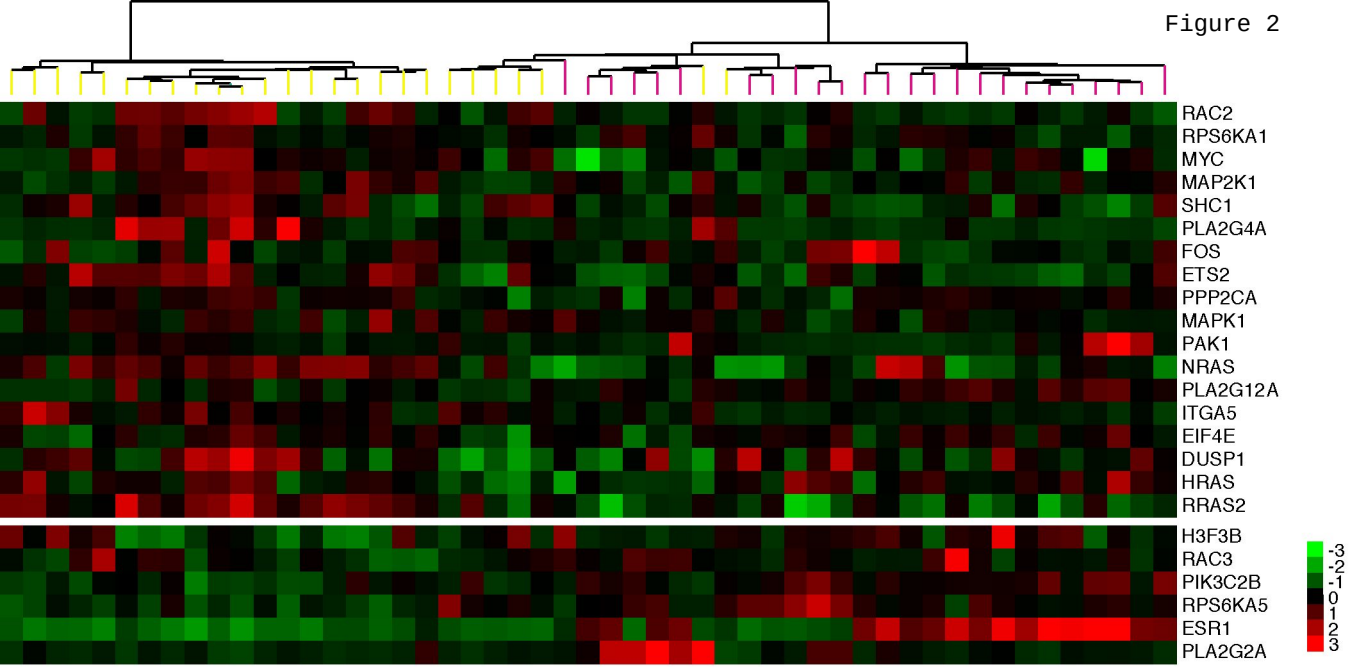
RAC2
RPS6KA1
MYC
MAP2K1
SHC1
PLA2G4A
FOS
ETS2
PPP2CA
MAPK1
PAK1
NRAS
PLA2G12A
ITGA5
EIF4E
DUSP1
HRAS
RRAS2
H3F3B
RAC3
PIK3C2B
RPS6KA5
ESR1
PLA2G2A
-3
-2
-1
0
1
2
3

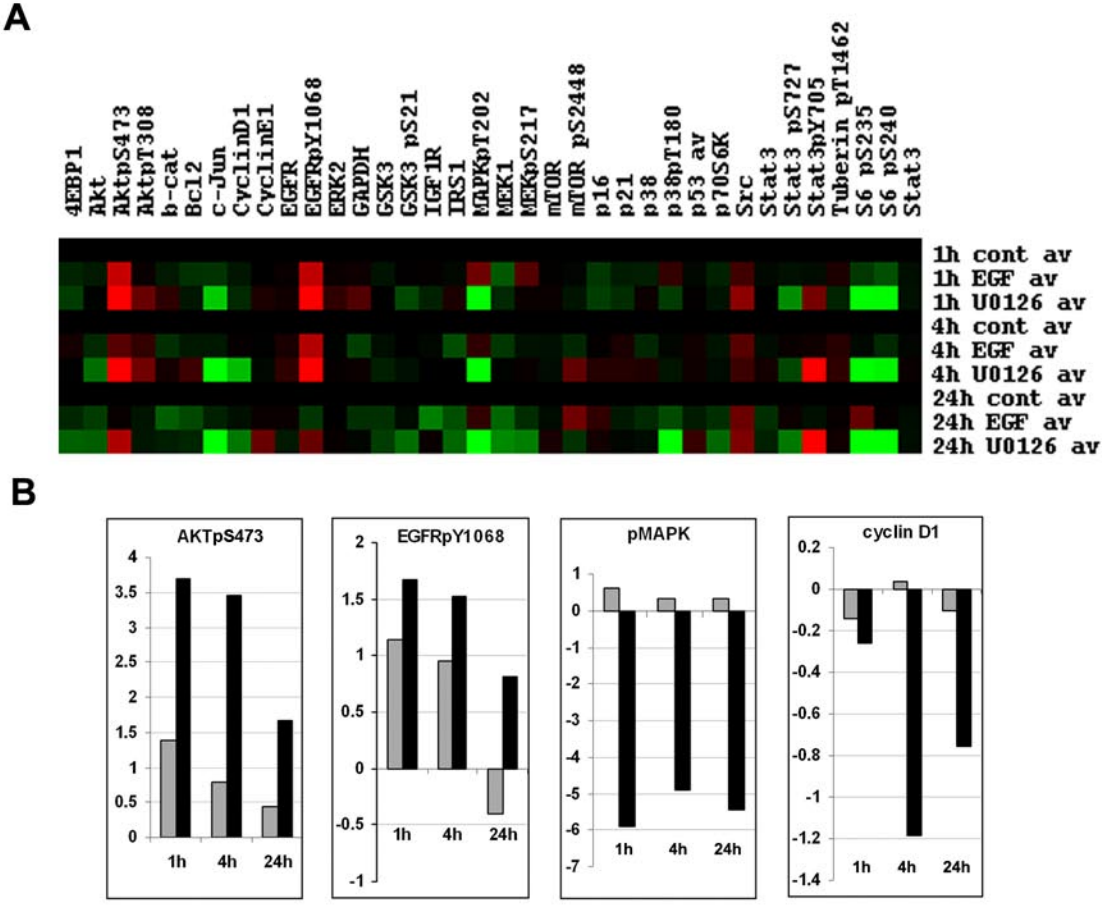
A
4EBP1
Akt
AktpS473
AktpT308
b-cat
Bcl2
c-Jun
CyclinD1
CyclinE1
EGFR
EGFRpY1068
ERK2
GAPDH
GSK3
GSK3 pS21
IGF1R
IRS1
MAPKpT202
MEK1
MEKpS217
mTOR
mTOR pS2448
p16
p21
p38
p38pT180
p53 av
p70S6K
Src
Stat3
Stat3 pS727
Stat3pY705
Tuberin pT1462
S6 pS235
S6 pS240
Stat3
1h cont av
1h EGF av
1h U0126 av
4h cont av
4h EGF av
4h U0126 av
24h cont av
24h EGF av
24h U0126 av
B
AKTpS473
EGFRpY1068
pMAPK
cyclin D1
1h
4h
24h
C
T47D
MDAMB231
1h
4h
EGF 10 ng/ml
U0126 10 uM
p-Akt S473
total Akt
p-Erk

Figure 3

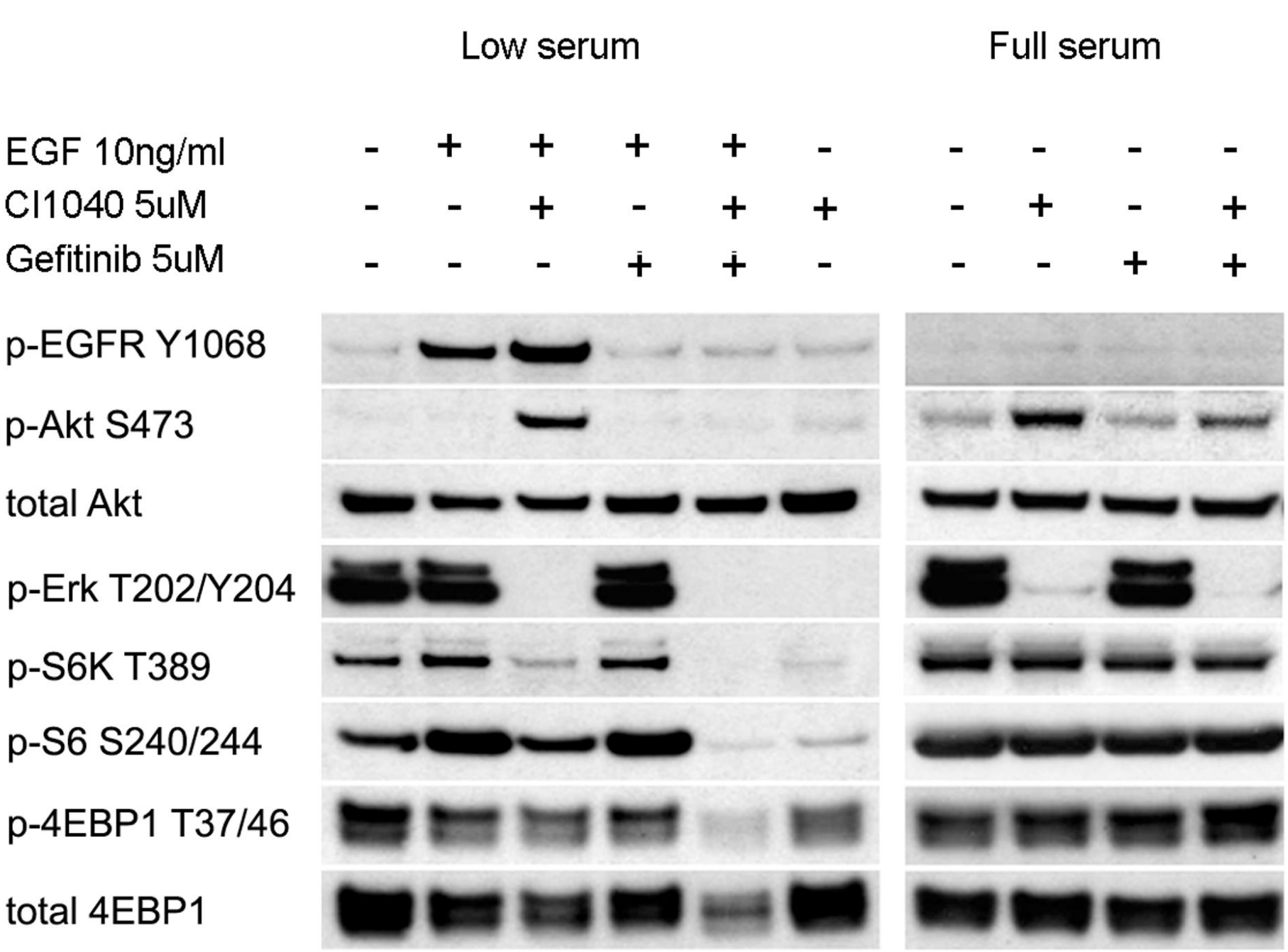
Low serum
Full serum
EGF 10ng/ml - + + + + - - - - -
CI1040 5uM - - + - + + - + - +
Gefitinib 5uM - - - + + - - - + +
p-EGFR Y1068
p-Akt S473
total Akt
p-Erk T202/Y204
p-S6K T389
p-S6 S240/244
p-4EBP1 T37/46
total 4EBP1

Figure 4

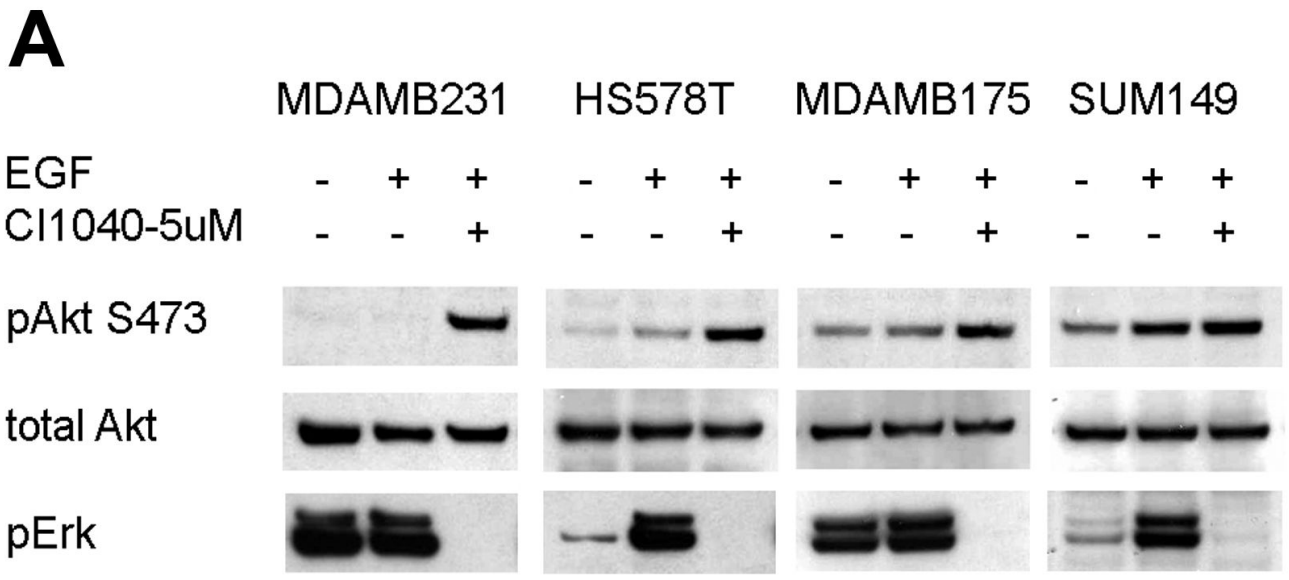
A
MDAMB231
HS578T
MDAMB175
SUM149
EGF
CI1040-5uM
pAkt S473
total Akt
pErk

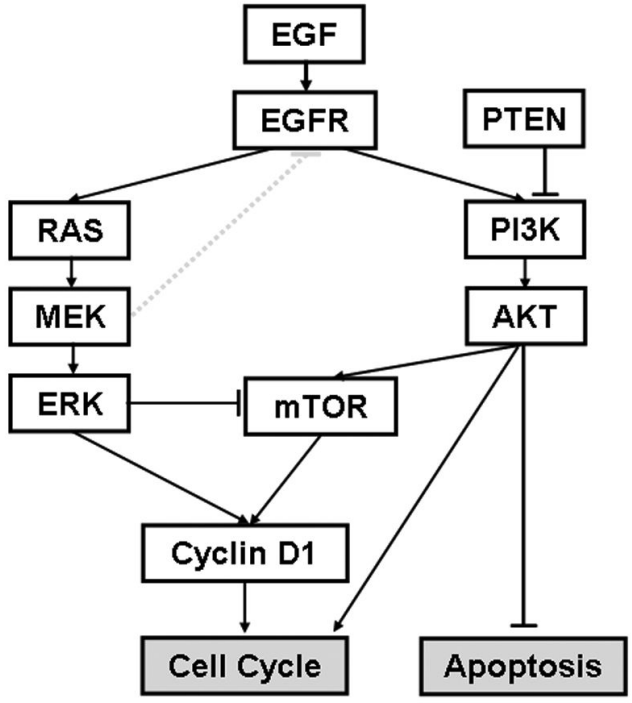
B
EGF
EGFR
PTEN
RAS
PI3K
MEK
AKT
ERK
mTOR
Cyclin D1
Cell Cycle
Apoptosis

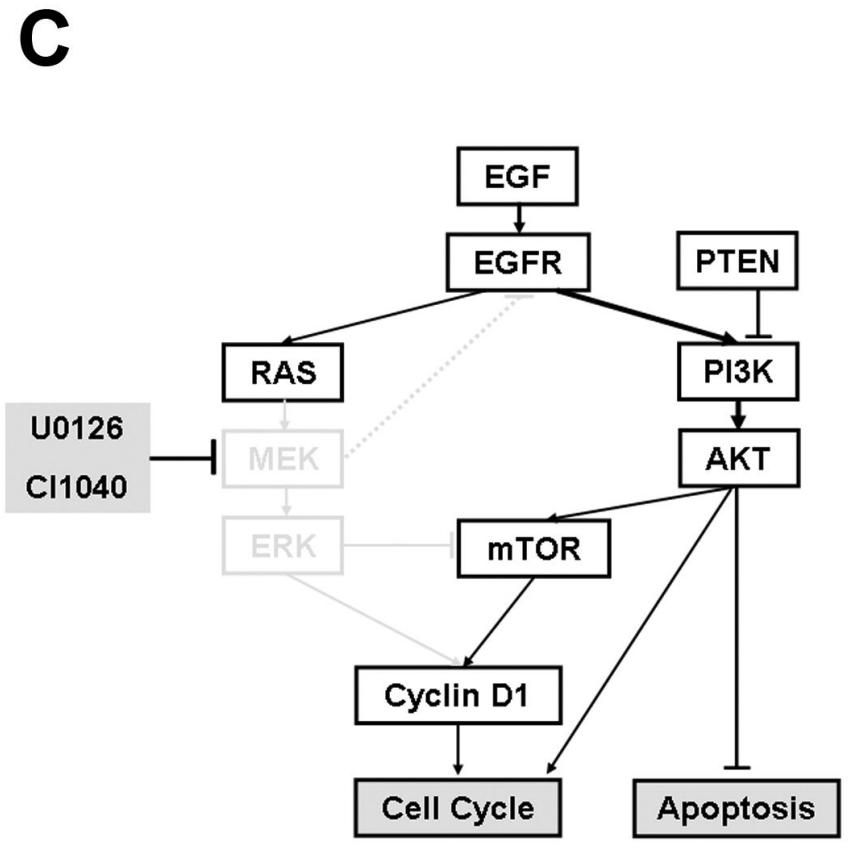
C
EGF
EGFR
PTEN
RAS
PI3K
U0126
CI1040
MEK
AKT
ERK
mTOR
Cyclin D1
Cell Cycle
Apoptosis

Figure 5

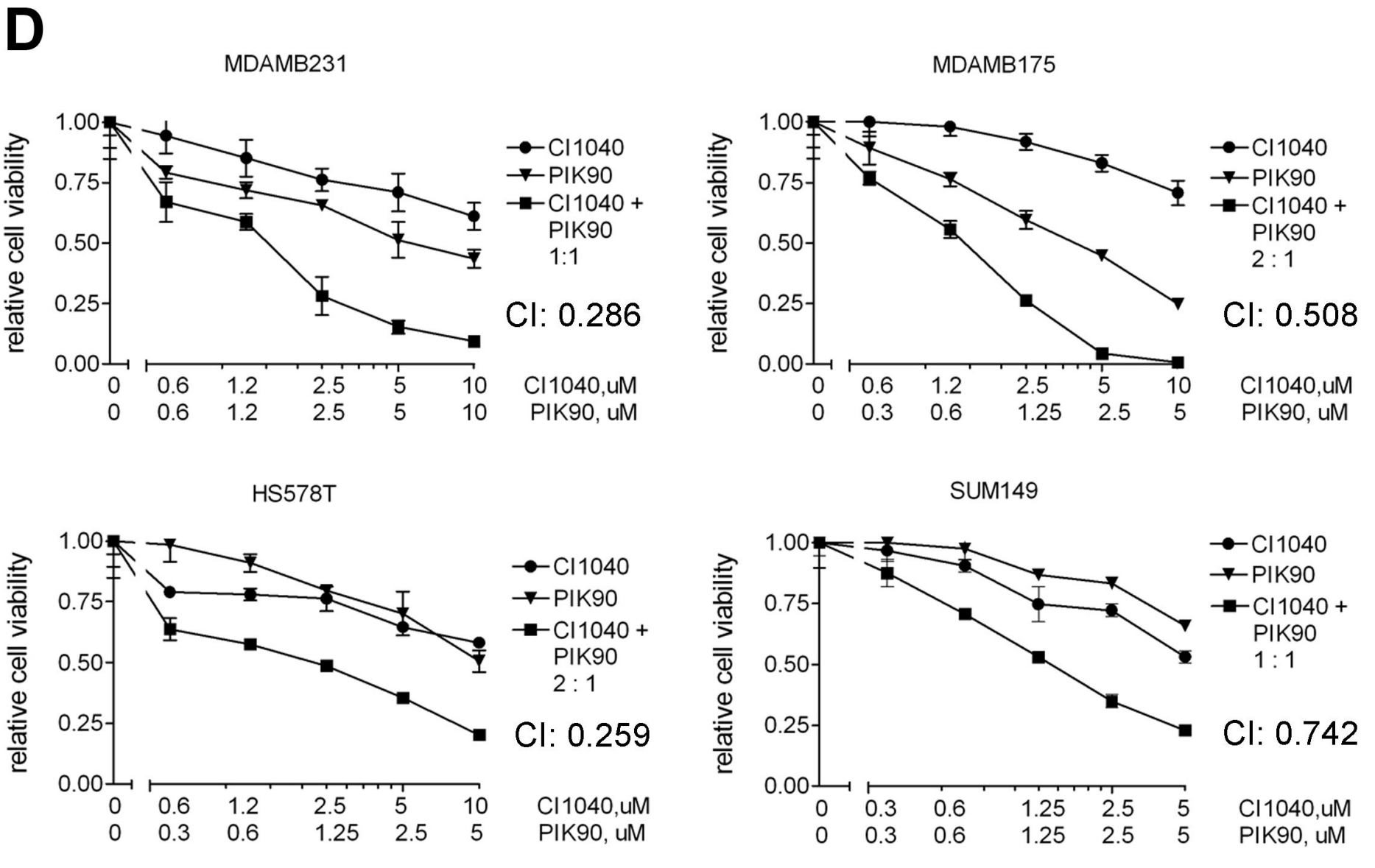
D
MDAMB231
relative cell viability
1.00
0.75
0.50
0.25
0.00
CI1040
PIK90
CI1040 + PIK90 1:1
CI: 0.286
0 0.6 1.2 2.5 5 10
CI1040,uM
0 0.6 1.2 2.5 5 10
PIK90, uM
MDAMB175
relative cell viability
CI1040
PIK90
CI1040 + PIK90 2 : 1
CI: 0.508
0 0.6 1.2 2.5 5 10
CI1040,uM
0 0.3 0.6 1.25 2.5 5
PIK90, uM
HS578T
relative cell viability
CI1040
PIK90
CI1040 + PIK90 2 : 1
CI: 0.259
0 0.6 1.2 2.5 5 10
CI1040,uM
0 0.3 0.6 1.25 2.5 5
PIK90, uM
SUM149
relative cell viability
CI1040
PIK90
CI1040 + PIK90 1 : 1
CI: 0.742
0 0.3 0.6 1.25 2.5 5
CI1040,uM
0 0.3 0.6 1.25 2.5 5
PIK90, uM

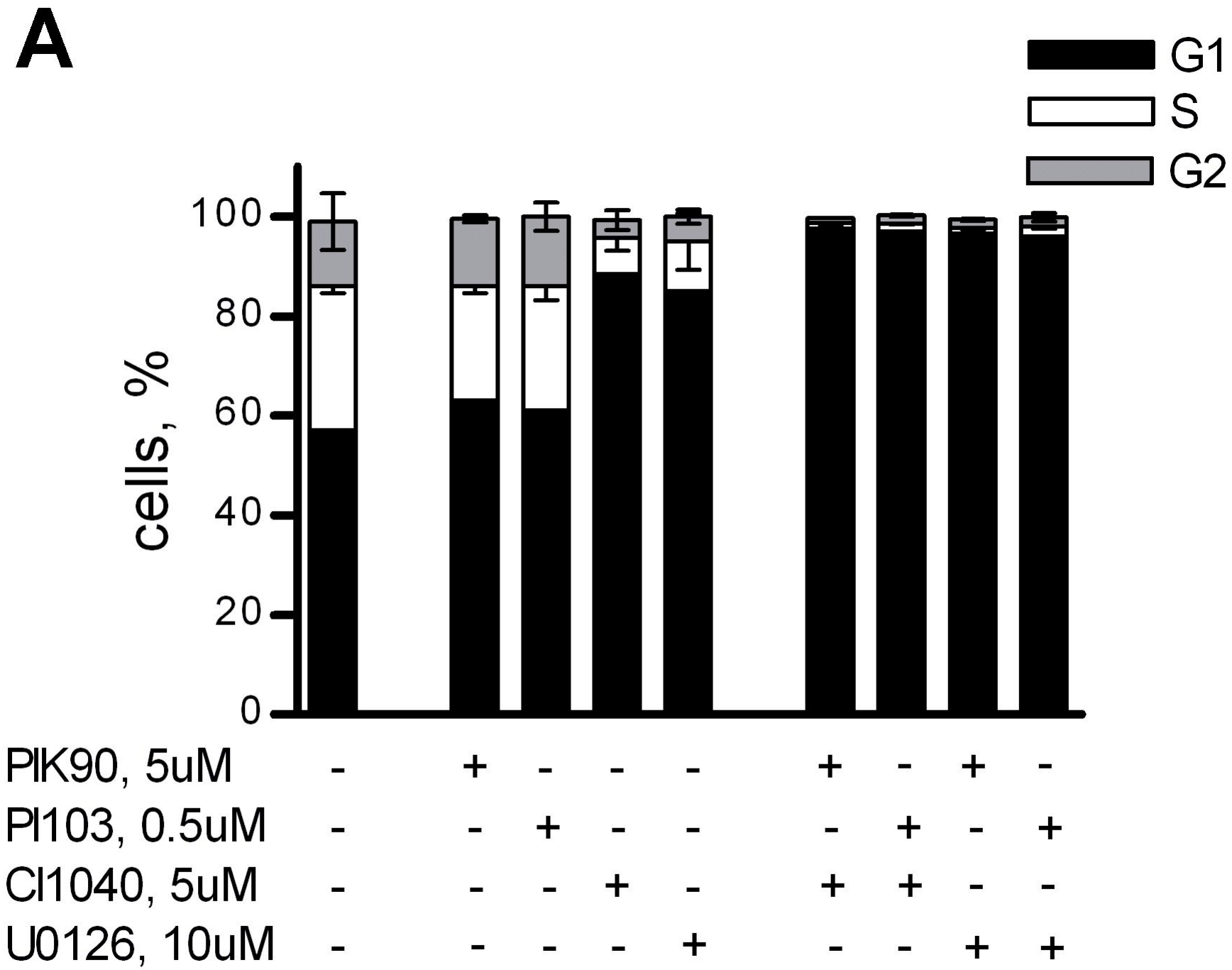
A
G1
S
G2
cells, %
100
80
60
40
20
0
PIK90, 5uM - + - - - + - + -
PI103, 0.5uM - - + - - - + - +
CI1040, 5uM - - - + - + + - -
U0126, 10uM - - - - + - - + +

Figure 6

B Western blot analysis

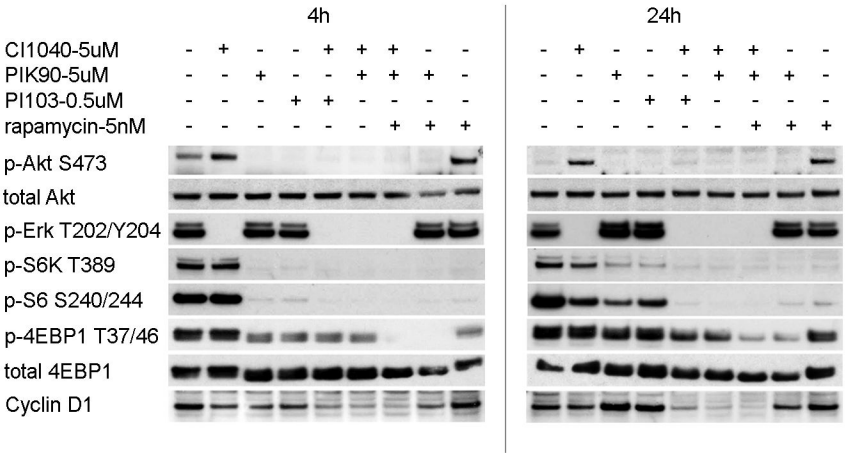

C TaqMan analysis of Cyclin D1 gene expression

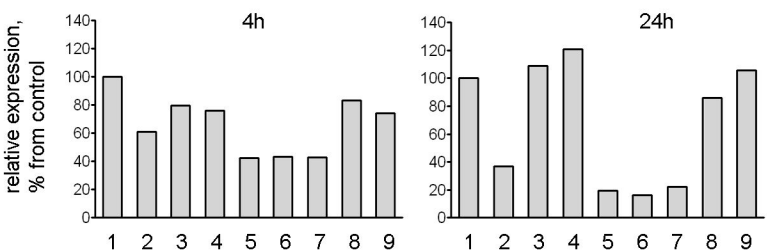

D

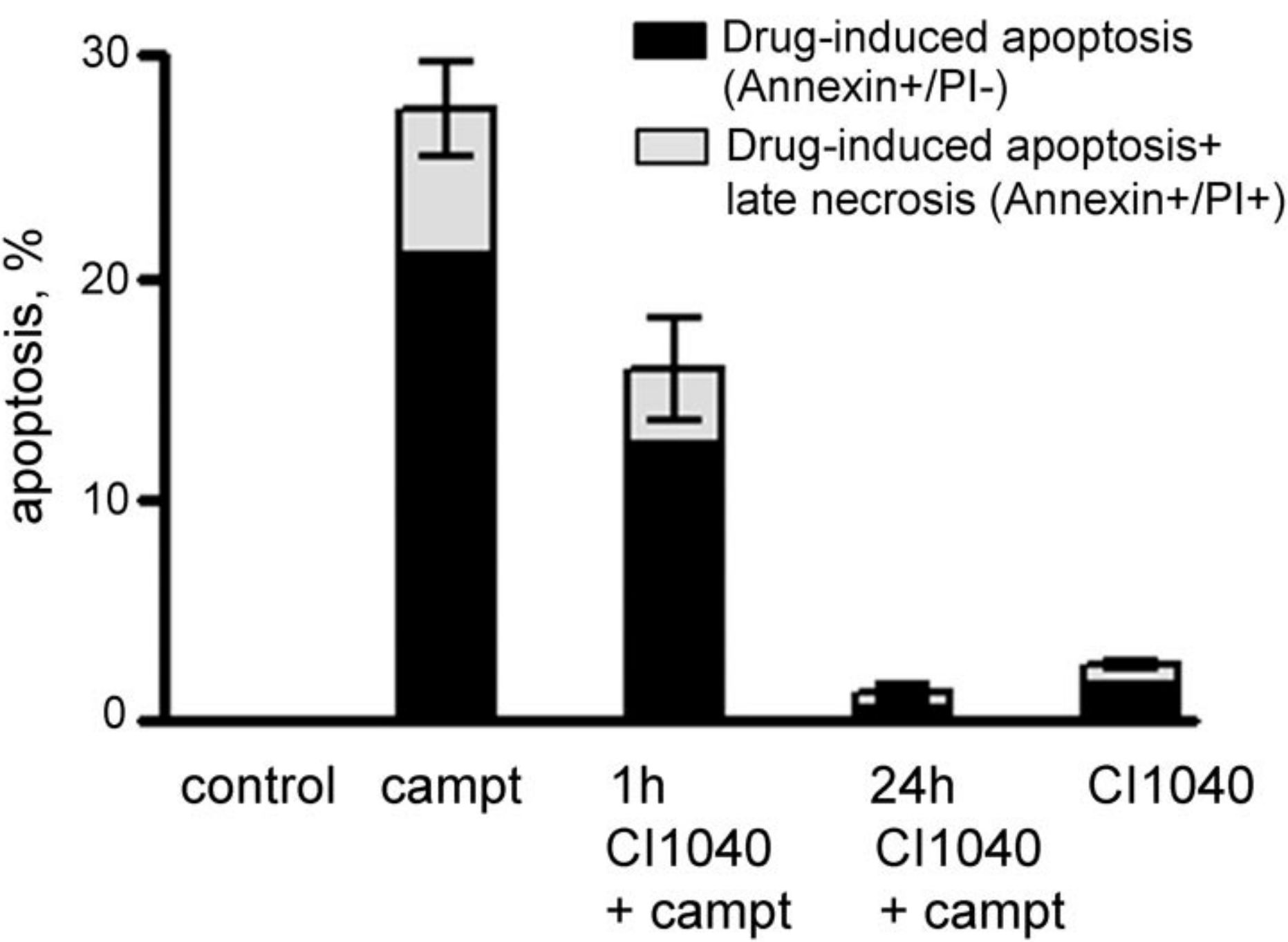
Drug-induced apoptosis (Annexin+/PI-)
Drug-induced apoptosis+ late necrosis (Annexin+/PI+)
apoptosis, %
30
20
10
0
control
campt
1h Cl1040 + campt
24h Cl1040 + campt
Cl1040